Alrtimi A, Rouainia M, Haigh S.

Thermal conductivity of a sandy soil.

***Applied Thermal Engineering* 2016, 106, 551-560**

Thermal conductivity of a sandy soil

A. Alrtimi[1], M. Rouainia[1] and S. Haigh[2]

[1]*Newcastle University, Newcastle NE1 7RU, UK*
[2]*The University of Cambridge, Schofield Centre, Cambridge, CB3 0EL*

Abstract

The thermal properties of soils are of great importance in many thermo-active ground structures such as energy piles and borehole heat exchangers. In this paper the effect of the porosity and degree of saturation on the thermal conductivity of a sandy soil that has not been previously thermally tested is investigated using steady state experimental tests. The steady state apparatus used in these tests was designed to provide high performance in controlling all boundary conditions. Twenty thermal conductivity experimental tests have been carried out at different porosity and saturation values. The performance of selected prediction methods have been validated against the experimental results. The validation shows that none of the selected models can be used effectively in predicting the thermal conductivity of Tripoli sand at all porosity and saturation values. However, some can provide good agreement at dry or nearly dry condition while others perform well at high saturations. The performance of most of the selected models also increases as the soil approaches a two phase state where conduction plays the dominant role in controlling heat transfer. An empirical equation of thermal conductivity expressed as a function of water content and porosity has been developed based on the experimental results obtained.

Keywords: Fine sand; Thermal conductivity; Steady state apparatus; Prediction models; Empirical models.

Corresponding author: M.Rouainia, Tel: +44 191 222 3608; Fax: +44 191 222 3522; Email: M.Rouainia@ncl.ac.uk

1. Introduction

Many engineering projects such as energy piles, borehole heat exchangers and underground oil/gas storage require heat transfer through soils to be considered in design. As shown in Fig. 1 by Johansen (1975), heat transfer in soils occurs due to several mechanisms. The relative importance of these mechanisms depends upon the volume fraction and thermal properties of the soil constituents, soil particles, water and air. Heat transfer in soils is normally dominated by conduction, with convection playing a significant role only in highly permeable soils, heat transfer due to vapour movement only being significant for soils with very low saturation and radiation being negligible. It is important to mention that the symbol k used in this work refers to the effective thermal conductivity which incorporates all forms of heat transfer that occur in the soil bulk. This is especially useful when dealing with porous material where different volumetric constituents of different materials are exist and different mechanisms of heat transfer occur. The major thermal properties that are of interest are thus the thermal conductivity and the thermal capacity. While it is possible to determine the heat capacity per unit volume of soil with fairly good accuracy using either analytical methods or experimentally using the calorimetric method, numerous problems are encountered in the determination of thermal conductivity (Kersten, 1949; Tarnawski et al., 2000; Nusier and Abu-Hamdeh, 2003). Soils are either two or three phase materials that consist of mineral particles, organic matter, and pores containing water, air or both. It is known that the thermal conductivity of the soil solids is higher than that of water and air. The thermal conductivity of soils has been found to be a function of several parameters including dry density, water content, mineralogy, temperature, particle size, particle shape and the volumetric proportions of the soil constituents. The thermal conductivity of soils can be determined either in the laboratory or in the field by transient or steady state methods. Steady state methods are considered more accurate than transient state methods (Farouki, 1986). It should be noted that inconsistent results have been obtained using the two methods. In some studies, the deviation reached as high as 50%, though, the average discrepancy between them is in the range of 10-20% (Midttomme and Roaldset, 1999; Abuel-Naga et al., 2009; Tang et al., 2008; Low et al., 2014). More concerns have been raised about the accuracy of transient methods related to the small variation in the current supplied during the test along with the effect of contact resistance which may lead to significant errors (Mitchell et al., 1987). In addition, the large diameter of the probe can be another source of error as the departure from the assumption of an infinitely thin probe may potentially cause

significant differences in estimation of the thermal conductivity due to the non-negligible heat storage and transmission in the needle probe itself (ASTM, 2008).

Steady state methods are time independent and measure the thermal conductivity when the heat flux through the soil reaches a constant level and the temperature of the soil specimen at any point remains constant with time. Steady state methods involve the production of a temperature difference between the sides of the soil specimen. Only the temperature drop across the specimen and the heat flux are needed to determine the thermal conductivity (Farouki, 1986). The main weakness of steady state methods is the long time required to reach the steady state condition, which allows moisture migration to take place from hot to cold regions. Various configurations of equipment have been established using steady state methods (Tan et al., 2006; Clarke et al., 2008). The efficiency of each apparatus is entirely dependent on the accurate estimation of the heat flux passing through the specimen cross-section which is mainly limited by the amount of the radial heat losses caused by the ambient temperature interference (ATI) along the specimen length.

In this paper, thermal conductivity measurements of Tripoli sand using a unidirectional heat flow steady state method will be presented. These experimental results will be used to evaluate common prediction models for the estimation of thermal conductivity.

2. Prediction methods

A range of equations exist in the literature for the prediction of thermal conductivity of sandy soils with varying saturation and dry density. Most of these equations were developed from empirical curve-fits to datasets. Therefore, they are likely to fit the data for which they were derived very well. Most of these datasets also comprise data solely from transient needle-probe measurements of soil's thermal conductivity where the thermal conductivity is determined by the theoretical solution of conductive heat flow from a line heat source method. Haigh (2012) and Dong et al. (2015) describe several of these models and assess their ability to predict the thermal conductivity of a wide range of soils whose thermal properties are available in the literature. They conclude that these models can either work only at a limited degree of saturation values or only applicable to certain soil types.

2.1. De Vries (1963) model

De Vries (1963) proposed a method that uses the weighted average of thermal conduc-

tivity value of each soil constituent. The De Vries' equation is based on the assumption of no contact between the soil particles and the values of the shape factor (g) assume that the soil particles have ellipsoidal shapes. The thermal conductivity according to De Vries is expressed as:

$$k = \frac{k_w x_w + F_a k_a x_a + F_s k_s x_s}{x_w + F_a x_a + F_s x_s} \tag{1}$$

where k_w, k_a, and k_s are the thermal conductivity of water, air and soil particles, respectively, x_w, x_a and x_s are the volume fraction of water, air and soil particles, respectively, and F_s and F_a are weighting factors depending on the shape and orientation of soil particles and air-pores respectively and equal to:

$$F_s = \frac{1}{3}\left[\frac{2}{1 + 0.125\big(k_s/k_w - 1\big)} + \frac{1}{1 + 0.75\big(k_s/k_w - 1\big)}\right] \tag{2}$$

$$F_a = \frac{1}{3}\left[\frac{2}{1 + g_a\big(k_s/k_w - 1\big)} + \frac{1}{1 + g_c\big(k_s/k_w - 1\big)}\right] \tag{3}$$

where g_a and g_c are shape factors defined by:

$$g_a = \begin{cases} 0.333 - x_{\frac{a}{n}}(0.333 - 0.035) & \text{for } 0.09 \leq x_w \leq n \\ 0.013 + 0.944 x_w & \text{for } 0 \leq x_w \leq 0.09 \end{cases} \tag{4}$$

and

$$g_c = 1 - 2g_a \tag{5}$$

where n is the porosity.

Another assumption assumed by De Vries (1963) is that the effective thermal conductivity of the air phase varies linearly with k_w due to humidity:

$$k_a = 0.0615 + 1.9 x_w \tag{6}$$

2.2. Johansen (1975) model

Johansen (1975) developed a method for determining the thermal conductivity of partially saturated soils based on the dry and saturated thermal conductivities when evaluated at same dry density. For natural dry soils, Johansen proposed the following empirical equation:

$$k_{dry} = \frac{0.135\gamma_{dry} + 64.7}{2700 - 0.94\gamma_{dry}} \pm 20 \tag{7}$$

here the dry density is given in kg/m^3, and the density of the soil solids is taken as 2700 kg/m^3.

For saturated soils, Johansen (1975) proposed a geometric mean equation based on the relative fraction of soil components and their thermal conductivities.

$$k_{sat} = k_s^{1-n} k_w^n \tag{8}$$

where n is the porosity, k_s is the soil solids' thermal conductivity, and k_w is the water's thermal conductivity.

In order to evaluate the unsaturated thermal conductivity in terms of k_{dry}, k_{sat} and degree of saturation S_r Johansen (1975) proposed the following correlation:

$$k = (k_{sat} - k_{dry})k_e + k_{dry} \tag{9}$$

where k_e is a function representing the influence of S_r on the thermal conductivity expressed as:

$$k_e = \begin{cases} 0.7 \log S_r + 1 & \text{when } S_r > 0.05 \quad \text{(coarse unfrozen soils)} \\ \log S_r + 1 & \text{when } S_r > 0.1 \quad \text{(fine unfrozen soil)} \end{cases} \tag{10}$$

2.3. Côté and Konrad (2005) model

Côté and Konrad (2005) modified the Johansen's model to eliminate the logarithmic reliance on saturation ratio that distorted predictions of the thermal conductivity at low degrees of saturations. The developed thermal conductivity model is based on the concept

of normalized thermal conductivity with respect to dry and saturated states. They offered a modified relationship of the form:

$$k = (k_w^n k_s^{1-n} - x10^{-\eta n})\left[\frac{aS_r}{1+(a-1)S_r}\right] + x10^{-\eta n} \tag{11}$$

where x and η account for particle shape effects, and a accounts for soil texture effect. For fine sand, they suggested $x = 3.55$, $\eta = 1.8$ and $a = 1.7$ W/mK.

2.4. Lu et al., (2007) model

Lu et al. (2007) also proposed a modification of Johansen's model. They proposed the following equation for the estimation of the thermal conductivity of sandy soils:

$$k = \left[k_w^n k_s^{1-n} - (b - an)\right] \exp\left[\alpha(1 - S_r^{\alpha-1.33})\right] + (b - an) \tag{12}$$

where a, b and α are empirical parameters. The values suggested for sandy soils are 0.56, 0.51 and 0.96, respectively.

2.5. Chen (2008) model

Based on a laboratory investigation of sandy soils, Chen (2008) proposed an empirical equation of thermal conductivity expressed as a function of porosity and degree of saturation. The equation is based on 80 needle-probe experimental tests on four types of sandy soils with different degrees of saturation at different porosities. He proposed the following equation:

$$k = k_w^n k_s^{1-n}\left[(1-b)S_r + b\right]^{cn} \tag{13}$$

where b and c are empirical parameters obtained from the fitting of the measured data and equal to 0.0022 and 0.78, respectively.

2.6. Haigh (2012) model

Haigh (2012) proposed an analytical model based on unidirectional heat flow through a three-phase soil element. The model analyses the one-dimensional heat flow between two equally sized spherical soil particles of radius R. two geometric parameters β and ξ are introduced to express the saturation degree and the void ratio respectively. According to the Haigh procedure, the overall thermal conductivity can be expressed as the following:

$$\frac{k}{k_s} = 2(1+\xi)^2\left[\frac{\alpha_w}{(1-\alpha_w)^2}\ln\frac{(1+\xi)+(\alpha_w-1)}{\xi+\alpha_w} + \frac{\alpha_a}{1-\alpha_a}\ln\frac{(1+\xi)}{(1+\xi)+(\alpha_a-1)x)}\right] + \frac{2(1+\xi)}{(1-\alpha_w)(1-\alpha_a)}\left[(\alpha_w-\alpha_a)x-(1-\alpha_a)\alpha_w\right] \quad (14)$$

where ξ, α and x are given by:

$$\xi = \frac{2e-1}{3} \quad (15)$$

$$\alpha = \frac{k_f}{k_s} \quad (16)$$

$$x = \frac{(1+\xi)}{2}\left(1+\cos\theta-\sqrt{3}\sin\theta\right) \quad (17)$$

where θ is given by:

$$\cos 3\theta = \frac{2(1+3\xi)(1-S_r)-(1+\xi)^3}{(1+\xi)^3} \quad (18)$$

and α_w and α_a are the thermal conductivities, normalised by that of the soil solids, of water and air respectively, as found in Eq. 16.

3. Experimental Methodology

3.1. Materials

The soil tested in this work is a sandy soil obtained from North Africa known as Tripoli sand. This sandy soil is found in a large area surrounding the city of Tripoli in Libya and also in many areas of the Sahara desert. The samples tested were extracted from a depth of one meter at a distance of 2.0 km south of the centre of Tripoli. Sieve analysis following BS (1377-2), indicates that this soil can be classified as a fine sand with coefficients of uniformity and curvature of 1.83 and 0.742, respectively (Fig. 2). It can be noted that 3.52% of Tripoli sand is fines. The mineralogical composition of this sample, determined by X-ray fluorescence, reveals that 93.25% of the soil solids are silica (Silicon Dioxide) with negligible amounts of other materials (Table 1).

3.2. Steady state thermal conductivity measurement

The thermal conductivity of the soil was measured at different degrees of saturation using a thermal cell that utilises the steady-state method (divided bar method). The design of the apparatus is based on the application of Fourier's law, where a one-directional uniform heat flux is generated through two identical specimens. The main body of the cell is made of acrylic, whose low thermal conductivity helps in minimising the radial heat loss and whose stiffness allows specimens to be compacted during preparation if required. The cell body consists of three main parts: a central insulating cylinder made from double-wall tubes separated by insulation material (40 mm of polyurethane foam) and two identical acrylic specimen cylinders, each having the same cross-section as the U100 sampling tube. Fig. 3 shows a schematic diagram of the thermal cell in which a heater disc is placed between the two specimens and a thermal gradient parallel to the axis of the specimen is generated by a DC cartridge rod heater that can be easily inserted into the disc through a drilled hole in the acrylic body of the cell. Two aluminium sink discs, at the unheated end of each specimen, were used to dissipate the heat from the outer ends of the specimens. The heater disc, sink discs and specimens have the same diameter (103 mm). In order to eliminate radial heat losses caused by ambient temperature interference (ATI), a thermal jacket surrounding the body of the cell was used. The thermal jacket consists of two spiral plastic tubes surrounding the body of the cell with one inlet in the middle and two outlets at the sides. Using a controlled temperature water bath and a circulating pump, the temperature of the thermal jacket can be adjusted to match the specimen temperature and hence reduce radial heat losses. More details on the apparatus design, performance and calibration are given by Alrtimi et al. (2014).

In steady state conditions, the temperature of at least three points for each specimen can be plotted against time. Using Fourier's equation for heat conduction assuming one dimensional heat flow at steady-state, the effective thermal conductivity, k, can be determined to be:

$$k = -\frac{Q\Delta L}{2A\Delta T} \quad [\mathrm{W/mK}] \tag{19}$$

where Q is the power supplied to the two samples, ΔT is the temperature drop across the specimen, ΔL is the specimen length and A is the cross sectional area.

3.2.1. Sample preparation

The study focused on the effects of degree of saturation and porosity on the thermal conductivity of Tripoli sand. For the interpretation of the test data, both porosity and degree of saturation were controlled. Four porosities (dry densities) were chosen (0.400, 0.430, 0.460, and 0.490), each level being tested at five degrees of saturation (0, 10, 25, 50, and 60 %). It should be noted that it was difficult to prepare samples with higher degree of saturations, especially at high porosities, as disaggregation occurs due to the elimination of the friction force between sand grains caused by the high water contents. This resulted in twenty tests being performed. The soil was first oven dried for 24hrs and allowed to cool in a dry place before being used. For each particular condition, the water content, dry density, and bulk density can be calculated using mass-volume relations. According to the desired moisture content, a dry soil mass was mixed with the appropriate amount of water. By knowing the volume of the specimen the required wet mass to obtain the predefined dry density can be calculated. The positions of the sink discs in the two specimen cylinders were adjusted to maintain the desired volume. The calculated wet masses of soil were then compacted in the two specimen cylinders using a conventional compaction procedure (Fig. 4). To ensure accurate assessment of the sample properties, the moisture content of the remaining portion of the samples were measured by dry method procedure and samples were reweighed to check the dry density. If the dry density was far from the required target, the preparation was repeated.

3.2.2. Test procedure

After preparation of the specimens was completed, the two cylinders containing the soil samples were then inserted into the insulating cylinder. The length of the specimen cylinders is designed to ensure complete contact between the heater disc and the two specimens when they reach their final position inside the insulating cylinder.

To monitor the temperature gradient along each specimen length, four thermocouples were laterally pushed through the lateral holes in the cell to reach the centre of the specimens at 0, 30, 60, and 80 mm from the heater. Two further thermocouples were used to monitor the temperature of the thermal jacket and room temperature. The room temperature was adjusted to the desired level (constant room temperature at 20^{o}C was applied for all tests). Fig. 5 shows the complete test setup. The apparatus then left for some time to allow soil specimens and the thermal cell to reach thermal equilibrium. This can be checked from continuous readings of thermocouple temperature. Once equilibrium

was achieved. The power selection depends on the required temperature gradient. For unsaturated conditions, the temperature gradient was kept as low as possible near the room temperature to avoid moisture migration. The power ($Q = V \times I$) supplied to the heater is controlled by changing the voltage V and current I supplied by the DC power supply Fig. 6 shows an example of data for temperature versus time. Using Eq. 19, the effective thermal conductivity k can be determined. At least two thermal conductivity values were calculated using different specimen lengths. The thermal conductivity results were then plotted against the corresponding specimen lengths. The radial heat losses along the specimen length can be identified by the slope of the line connecting these thermal conductivity values. If the line is not horizontal, radial heat losses took place during the test period. A correction step can be applied by extrapolating the thermal conductivities to a specimen length of zero (Alrtimi et al., 2014). Fig. 7 shows an example of the thermal conductivity correction method.

4. Experimental results and discussion

The thermal conductivities of twenty specimens of Tripoli sand with different porosities and degrees of saturation have been measured using the steady state apparatus method. The physical properties of the tested specimens and the effective thermal conductivities obtained are presented in Table 2. From these results, several relations between the physical properties of Tripoli sand and thermal conductivity can be assessed. The effect of other properties such as mineralogical composition and grain size cannot be evaluated as they were identical in all tests. Furthermore, the performance of selected prediction models results was evaluated against the experimental results to establish the validity of using such models in the calculation of the thermal conductivity of the selected Tripoli sand.

4.1. Steady state method versus prediction models

A comparison between the experimental results obtained using the steady state thermal cell apparatus and the corresponding values obtained from the selected prediction methods is shown in Fig. 8. It should be noted that in all calculations the values of thermal conductivity of the solids (quartz), water, and air were taken as 7.69, 0.60 and 0.026 W/mK respectively. These values are obtained from Horai (1971), Ramires et al. (1995) and Stephan et al. (1985), respectively.

It can be seen that the De Vries (1963) model can be used to satisfactorily predict the thermal conductivity of Tripoli sand at high degrees of saturation. However, at low saturation levels, the model predicted higher values than were observed experimentally. This may be attributed to the assumption that the soil particles and air are considered to be immersed in a continuous water phase. This assumption is only valid only at high water content. The Johansen (1975) model is not able to predict the thermal conductivity of Tripoli sand at dry condition. The main reason of that is the logarithmic dependence on the saturation ratio which leads to erroneous results at low degrees of saturation. However, at high saturations (above 50%) the model values are in good agreement with the experimental results with a deviation ranging between 8 and 19% from experimental results depending on the porosity level. The Côté and Konrad (2005) model correctly predicted the thermal conductivity of Tripoli sand at dry condition for all levels of porosity with an average deviation less than 8%. This was also observed at high saturations with average deviation around 13%. It can also be observed from Fig. 8, that the same result is captured by Lu et al. (2007). This is due to the fact that both models can be seen as a logical extension of Johansen's model. It should be mentioned that for the Lu et al. (2007) model, the optimum fit to all test results is obtained with values $a = 2.71$ and $b = 1.65$ for the relationship between dry thermal conductivity and porosity. Fig. 8 shows that the Chen (2008) model overestimated the result of thermal conductivity at dry and low degrees of saturation of Tripoli sand with a deviation ranging from 30 to 50%. However, at high saturations the results became more consistent, especially at low porosities, and the deviation ranged between 6 to 22%. The equations derived by Haigh (2012) are relatively complicated when compared with existing empirical models. The model simplifies the fluid behavior at particle contacts at various void ratios and soil saturations. The results obtained from the application of this theoretical model for Tripoli sand shows that this model can only provide reasonable results at low porosity values especially at high degrees of saturation.

From these observations, it can be concluded that none of the selected models is able to correctly match the thermal conductivity of Tripoli sand at all conditions. It is obvious that some of these models give good predictions in relatively dry conditions and others at high degrees of saturation. One important observation is that most of these models are able to produce better predictions at high saturation and low porosity. This implies that performance increases as the soil approaches a two phase state where conduction plays the dominant role in controlling heat transfer. It is also noticeable that all models relatively

failed to estimate the thermal conductivity of such soil at low degrees of saturation. This might be due to the lack of the consideration of some key governing factors such as soil and liquid type and pore size distribution in these models (Dong et al., 2015). The calculated thermal conductivity using these prediction methods is compared against the measured values in Fig. 9. The observed discrepancies between the calculated and measured thermal conductivity results can be explained by the fact that most of the presented models were developed from empirical curve-fit datasets for soils with different physical properties. Furthermore, the values quoted for thermal conductivity of the soil particles vary from one model to another. The true thermal conductivity of soil grains will obviously impact on the effective thermal conductivity of the bulk soil. Finally, most of the experimental results used in the calibration of these models were based on transient methods which provide different values of thermal conductivity when compared with steady state methods. Midttomme and Roaldset (1999) state that up to 20% difference between the two methods has been observed in previous studies.

The observed overall higher thermal conductivity of Tripoli sand can be related to the existence the clay fraction (3.52%). Despite the much lower thermal conductivity of clay compared with the quartz grains, at low moisture contents the clay provides more thermal bridges between the granular skeleton of sand which increase conductive heat flow at the particle contacts (Sakaguchi et al., 2007).

4.2. Effect of degree of saturation

For a given porosity (dry density), Fig. 10 clearly shows that the thermal conductivity increases as the degree of saturation increases. This trend is most significant at low saturation ratios, (less than 10%). After that the increase decelerates with parallel trend for all levels of porosity. When the thermal conductivity results are plotted against the water content (see Fig. 11), the thermal conductivity at first increases rapidly as the moisture content increases but beyond a certain moisture content, (approximately 3%), the rate of the increase become much lower. In dry conditions, owing to the thermal conductivity of air being much lower than that of the other soil components, heat transfers only through contact points between soil particles resulting in a low thermal conductivity. As the water content increases, more water collects around the contact points and forms water bridges between soil grains. As a result, the inter-particle contact within the material is enhanced by the formation of the water menisci and so conduction from one grain to another is enhanced (Tarnawski et al., 2000; Hall and Allinson, 2009). This improvement is rapid

until the water film covers all the surface of the soil particles. At this point, the transfer of heat arises largely from two mechanisms; one is heat conduction through the soil skeleton and water between solid particles (thermal bridges), and the other is the transfer of latent heat. Under a temperature gradient, more water vapor is likely to condense on the water films surrounding the soil particles due to the larger surface area of the water films compared with that of the water bridges. Condensation, conduction and evaporation take place through both the water films and the water bridges (Sakaguchi et al., 2007). Both heat conduction through the water bridges and the latent heat transferred with the movement of water vapor are the main cause of the rapid enhancement of the effective thermal conductivity at low water content values. Beyond this point, any enhancement of the thermal conductivity is only related to the replacement of air by water in the pore spaces, resulting in a slower increase in thermal conductivity.

4.3. Effect of dry density

The overall effective thermal conductivity of a porous medium can be expressed as the sum of the conductivities related to different heat transfer processes. In dry soils, the effective thermal conductivity is mainly controlled by the gaseous phase (Huetter et al., 2008). This is because the contact areas between the particles are very small compared to the contact areas between air and particles. Heat transfer is hence governed by conduction within the gas and by heat transfer across the gas-solid interface. The thermal conductivity of dry soils is hence usually low owing to the low thermal conductivity of air. This can be observed clearly in Fig. 12, showing the variation of thermal conductivity with dry density at different degrees of saturation. It can also be observed that dry density has a much more minor impact on thermal conductivity than does the degree of saturation. Increasing dry density results in a minor increase in thermal conductivity owing to a slight increase in the number of contact points between soil particles (Hall and Allinson, 2009). The parallel lines in Fig. 12 indicate that the effect of dry density is similar at all degrees of saturation in Tripoli sand.

5. The proposed empirical model for Tripoli sand

From the above discussion it obvious that none of the selected prediction models can be used effectively in determining of the Tripoli sand thermal conductivity. An empirical equation based on the experimental results can be produced that can be used to better

predict thermal conductivity. The results obtained from the steady state apparatus are adopted in this empirical model.

From the relation between the thermal conductivity and water content that was presented in Fig. 11 it can be observed that the thermal conductivity of Tripoli sand can be satisfactory described as a logarithmic function of the water content. Fig. 13 is an example of this logarithmic relation. This logarithmic function can be determined at all levels of porosity with R^2 values between 0.9694 to 0.9732. Accordingly, the effective thermal conductivity of Tripoli sand can be expressed in terms of water content as:

$$k = a \ln w + b \tag{20}$$

where a and b are empirical values expressing the effect of the porosity. Table 3 shows the values of a and b at different porosities. From this table, the empirical parameters a and b can be expressed in terms of porosity, n, as:

$$a = 1 - n \quad \text{and} \quad b = 6.83 - 7.75n \tag{21}$$

Substituting in Eq. 20 we obtain:

$$k = (1 - n) \ln w - 7.75n + 6.83 \tag{22}$$

Under dry conditions, the following linear relation between the effective thermal conductivity and the dry density ρ_{dry} can be used:

$$k = 1.025\rho_{dry} - 1.065 \tag{23}$$

The calculated thermal conductivity values using this equation are compared to the experimental results in Fig. 14 and the implementation of this model using different Tripoli sand conditions along with corresponding experimental results are shown in Fig. 15. From these figures, it is clear that this model can provide sensible values of Tripoli sand thermal conductivity with average variation from experimental results equal to 5.734%.

6. Conclusion

This paper presented results of an experimental program carried out on sandy soil aiming to investigate the thermal behaviour of this soil under different porosities and

degrees of saturation. The thermal conductivity has been measured using a recently developed steady state apparatus. The design of the steady state apparatus is based on the application of Fourier's law where a one-directional uniform heat flux is generated through two identical specimens. The results have shown that the thermal conductivity increases significantly below a certain level of saturation and started to decelerate above this level. The validation of some selected prediction models against the experimental results revealed that none of these models can be used to predict the thermal conductivity of such soil at all conditions. Some can provide good agreement at dry or nearly dry condition while others perform well at high saturations. It is also notable that most of the prediction models provided better results at low levels of porosity, especially at high saturation ratio. The experimental results have also shown that the variation of the thermal conductivity against the volumetric water content can be closely expressed as a logarithmic function. As a result, an empirical model based on the experimental results expressing the effective thermal conductivity in terms of water content and porosity has been obtained and validated.

References

Johansen, O. 1975. Thermal conductivity of soils. PhD thesis, Trondheim, Norway, ADA 044002.

Kersten, M.S. 1949. Laboratory research for the determination of the thermal properties of soils. Bulletin 28, Engineering Experiment Station, University of Minnesota, Minneapolis.

Tarnawski, V.R., Leong W. H. and Bristow K. L. 2000. Developing a temperature-dependent Kersten function for soil thermal conductivity. Int. J. of Energy Research 24, 15.

Nusier, O.K. and Abu-Hamdeh, N.H. 2003. Laboratory techniques to evaluate thermal conductivity for some soils. Heat and Mass Transfer 39(2), 119-123.

Farouki. 1986. Thermal properties of soil, Series on Rock and Soil Mechanics. Germany: Trans Tech publication.

Midttomme, K. and Roaldset, E. 1999. Thermal conductivity of sedimentary rock: uncertainties in measurement and modelling. The geological Society of London 158, 45-60.

Abuel-Naga, H.M., Bergado, D.T., Bouazza, A. and Pender, M.J. 2009. Thermal conductivity of soft Bangkok clay from laboratory and field measurements. Engineering Geology 105(3-4), pp. 211-219.

Low, J.E., Loveridge, F.A., Powrie, W., Nicholson, D. 2014. A comparison of laboratory and in situ methods to determine soil thermal conductivity for energy foundations and other ground heat exchanger applications. Acta Geotechnica 10, 209-218.

Tang A-M., Cui Y-J., Le T.T. 2008. A study on the thermal conductivity of compacted bentonites. Applied Clay Science 41, 181-189.

Mitchell, J.K., Kao, T.C. 1978. Measurement of soil thermal resistivity. J. Geotech. Geoenviron. Eng, 104(10), 1307-1320.

ASTM 2008. A testing method for determining the thermal conductivity of soils and soft rocks by a thermal needle probe procedure. D 5334.

Tan, J.C., Tsipas, S.A., Golosnoy, I.O., Curran, J.A., Paul, S. and Clyne, T.W. 2006. A steady-state Bi-substrate technique for measurement of the thermal conductivity of ceramic coatings. Surface and Coatings Technology 201(3-4), 1414-1420.

Clarke, B.G., Agab, A. and Nicholson, D. 2008. Model specification to determine thermal conductivity of soils. Proc. of the Institution of Civil Engineers: Geotechnical Engineering 161(3), 161-168.

Haigh, S.K. 2012. Thermal conductivity of sands. Geotechnique 62(7), 617-625.

Dong, Y., McCartney, J. S., and Lu, N. 2015. Critical review of thermal conductivity models for unsaturated soils. Geotech. Geol. Eng., 1-15.

De Vries, D.A. 1963. Thermal properties of soil. in: van Wijk, W.R., (Eds.),Physics of plant environment. Amsterdam, New Holland, pp. 210-235.

Côté, J. and Konrad, J.M. 2005. A generalized thermal conductivity model for soils and construction materials. Canadian Geotechnical Journal 42(2), 443-458.

Lu, S., Ren, T., Gong, Y. and Horton, R. 2007. An improved model for predicting soil thermal conductivity from water content at room temperature. Soil Science Society of America Journal 71(1), 8-14.

Chen, S. 2008. Thermal conductivity of sands. Heat and Mass Transfer 44(10), 1241-1246.

BS 1377-1:1990. Methods of test for soils for civil engineering purposes General requirements and sample preparation.

Alrtimi A., Rouainia M., Manning , D.A.C. 2014. An improved steady-state apparatus for measuring thermal conductivity of soils. Int. J. of Heat and Mass Transfer 72, 630-636.

Horai, K.I. 1971. Thermal conductivity of rock-forming minerals. Journal of Geophysical Research, 76(5), 1278-1308.

Ramires, M.L.V., Nieto de Castro, C.A., Nagasaka, Y., Nagashima, A., Assael, M.J., Wakeham, W.A. 1995. Standard reference data for the thermal conductivity of water. J. Phys. Chem. Ref. Data 24, 1377-1381.

Stephan, K., Laesecke, A. 1985. Thermal conductivity of fluid air. J. Phys. Chem. Ref. Data 14(1), 227-234.

Tarnawski, V.R., Gori, F., Wagner, B. and Buchan, G.D. 2000. Modelling approaches to predicting thermal conductivity of soils at high temperatures. Int. J. of Energy Research 24(5), 403-423.

Hall, M. and Allinson, D. 2009. Assessing the effects of soil grading on the moisture content-dependent thermal conductivity of stabilised rammed earth materials. Applied Thermal Engineering 29(4), 740-747.

Sakaguchi, I., Momose, T. and Kasubuchi, T. 2007. Decrease in thermal conductivity with increasing temperature in nearly dry sandy soil. European Journal of Soil Science 58(1), 92-97.

Huetter, E.S., Koemle N. I., G. Kargl and Kaufmann, E. 2008. Determination of the effective thermal conductivity of granular materials under varying pressure conditions. Journal of Geophysical research, 113(E12).

List of Tables

Table 1: Mineralogical composition of Tripoli sand.

SiO_2 (%)	TiO_2 (%)	Al_2O_3 (%)	Fe_2O_3 (%)	MnO (%)	MgO (%)	CaO (%)	Na_2O (%)	K_2O (%)	P_2O_5 (%)	SO_3 (%)
93.25	0.202	2.61	0.95	0.012	0.17	1.04	0.24	1.04	0.019	<0.002

Table 2: Physical properties and the corresponding effective thermal conductivities.

Test	ρ_{dry}	e	n	S_r	w	k (W/mK)	
	(g/cm^3)	-	(%)	(%)	(%)	Steady	Transient
1	1.344	0.972	0.493	0.015	00.55	0.348	0.180
2	1.353	0.959	0.490	0.106	03.83	1.596	1.141
3	1.350	0.963	0.491	0.251	09.13	1.830	1.437
4	1.343	0.974	0.493	0.493	18.10	2.052	1.829
5	1.315	1.015	0.504	0.548	21.00	2.151	1.918
Average	1.340	0.978	0.494				
6	1.425	0.859	0.462	0.014	00.44	0.352	0.194
7	1.430	0.853	0.460	0.108	03.46	1.701	1.361
8	1.434	0.849	0.459	0.240	07.67	1.941	1.689
9	1.425	0.859	0.462	0.488	15.84	2.135	2.132
10	0 1.412	0.877	0.467	0.575	19.03	2.283	2.226
Average	1.425	0.859	0.462				
11	1.503	0.763	0.433	0.017	00.48	0.454	0.215
12	1.519	0.745	0.427	0.104	02.92	1.669	1.383
13	1.513	0.752	0.429	0.244	06.92	2.060	1.960
14	1.503	0.763	0.433	0.479	13.80	2.216	2.213
15	1.482	0.788	0.441	0.559	16.63	2.352	2.339
Average	1.504	0.762	0.432				
16	1.580	0.677	0.404	0.023	0.60	0.584	0.238
17	1.579	0.678	0.404	0.098	02.52	1.679	1.606
18	1.589	0.668	0.401	0.254	06.41	2.153	2.034
19	1.578	0.680	0.405	0.487	12.48	2.325	2.321
20	1.552	0.707	0.414	0.565	15.08	2.475	2.469
Average	1.575	0.682	0.406				

Table 3: Values of empirical parameters a and b at different porosities.

Porosity n	Parameter a	Parameter b
0.4940	0.4821	2.9578
0.4622	0.4992	3.1660
0.4325	0.5250	3.3589
0.4055	0.5691	3.6094

List of Figures

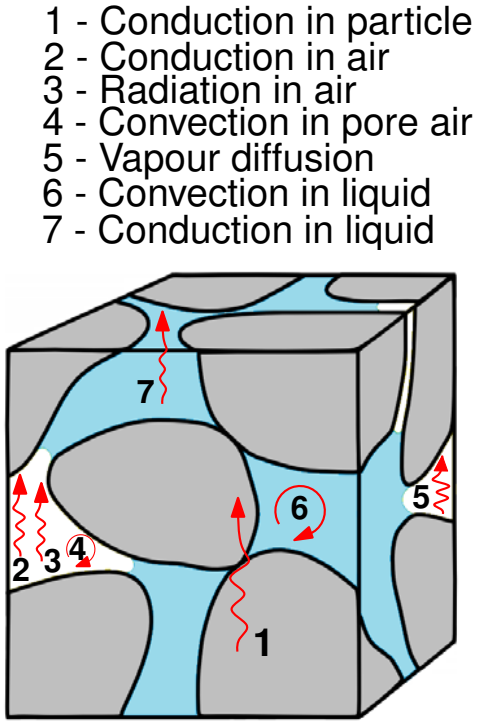

Figure 1: Heat transfer paths in soil mass material.

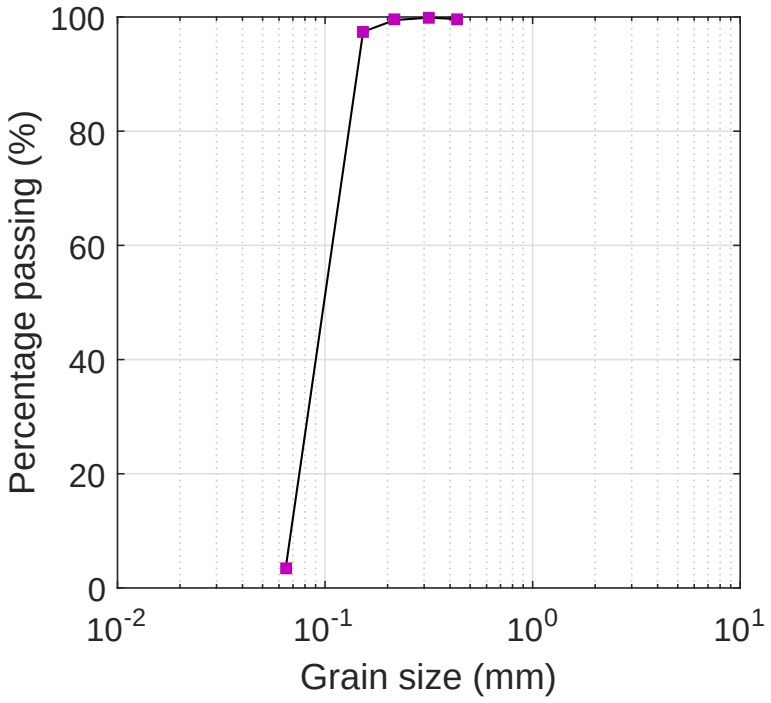

Figure 2: Grain size distribution for Tripoli sand.

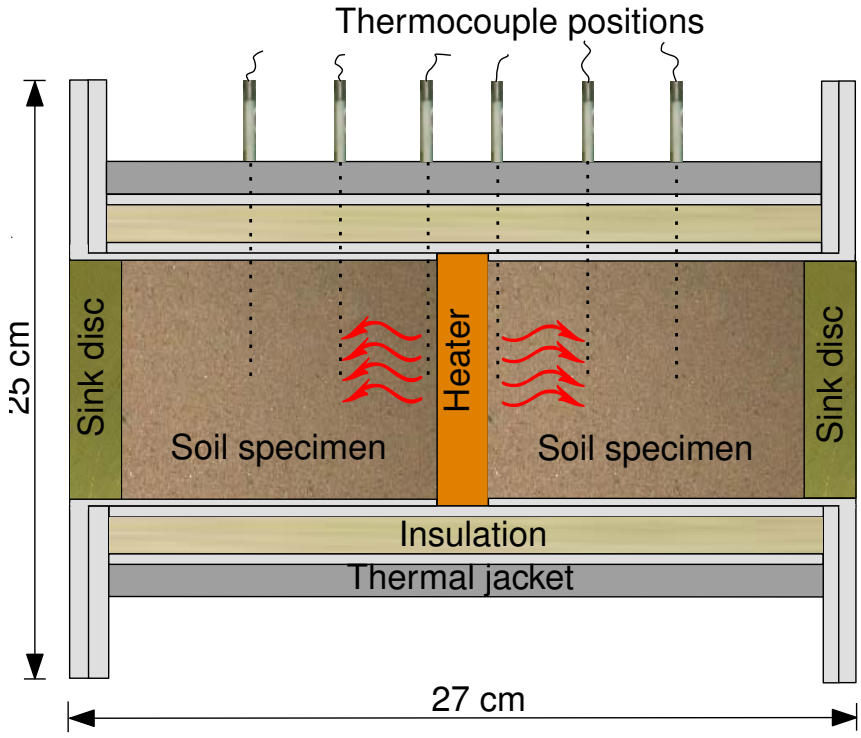

Figure 3: Steady state thermal cell setup.

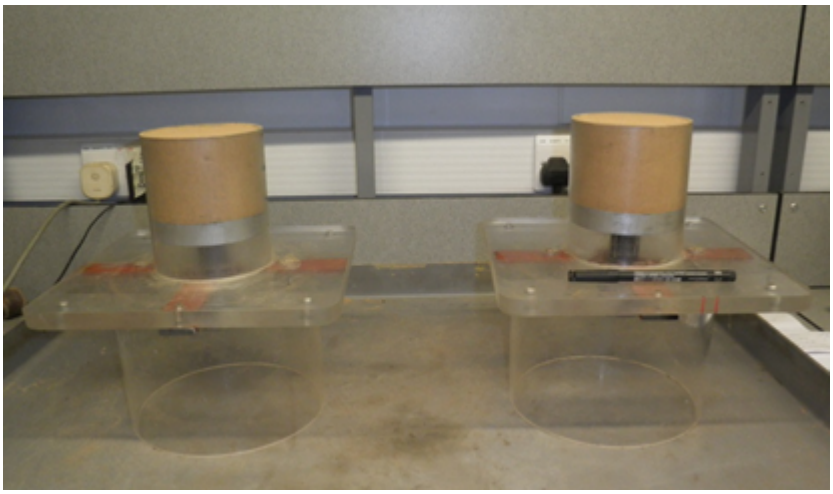

Figure 4: Two specimens containing compacted Tripoli sand samples.

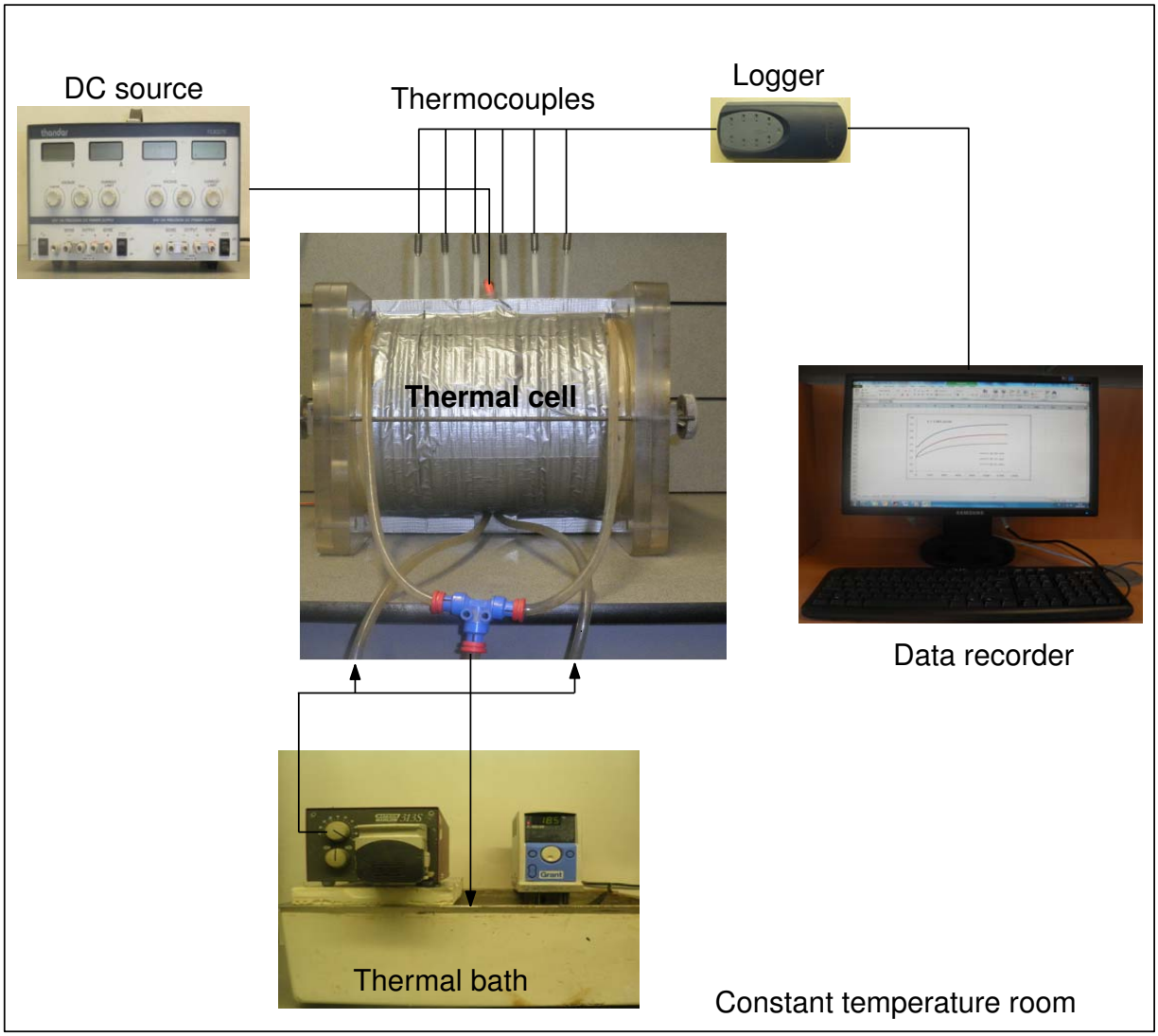

Figure 5: Complete thermal cell setup.

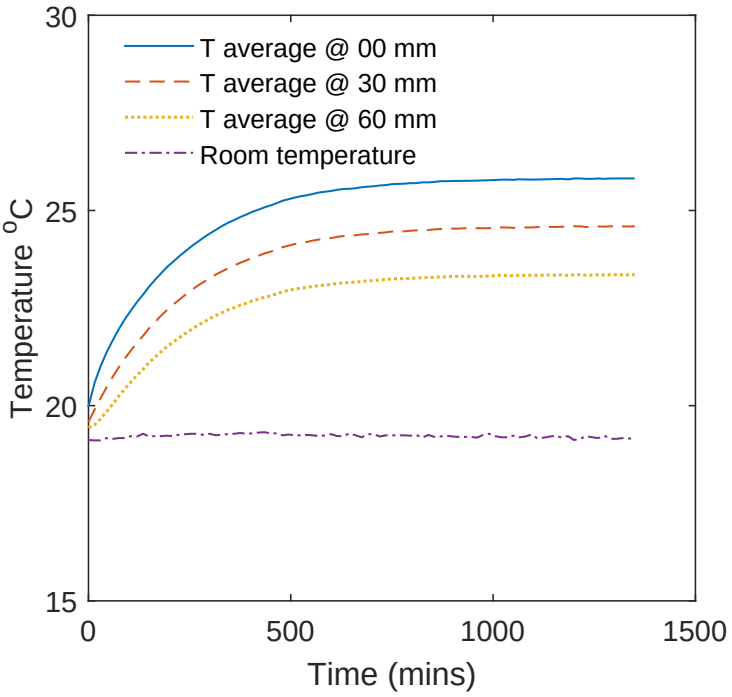

Figure 6: Example of temperature versus time curve along the specimen length

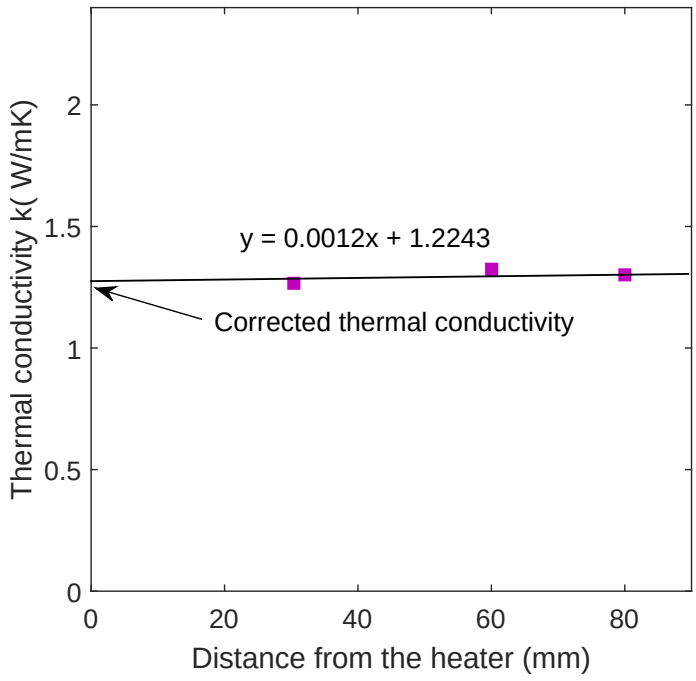

Figure 7: Example of thermal conductivity correction method.

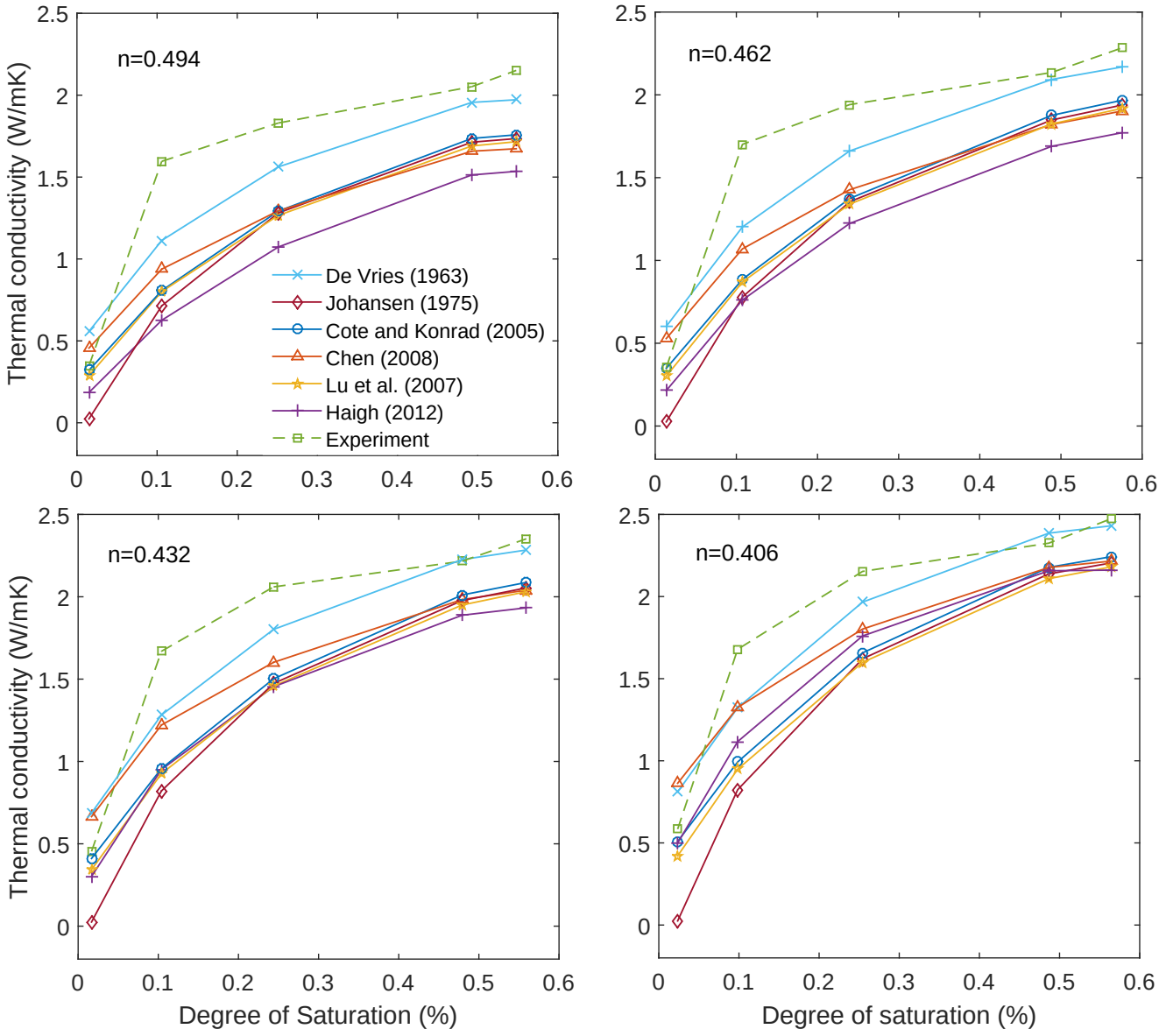

Figure 8: Experimental versus prediction results .

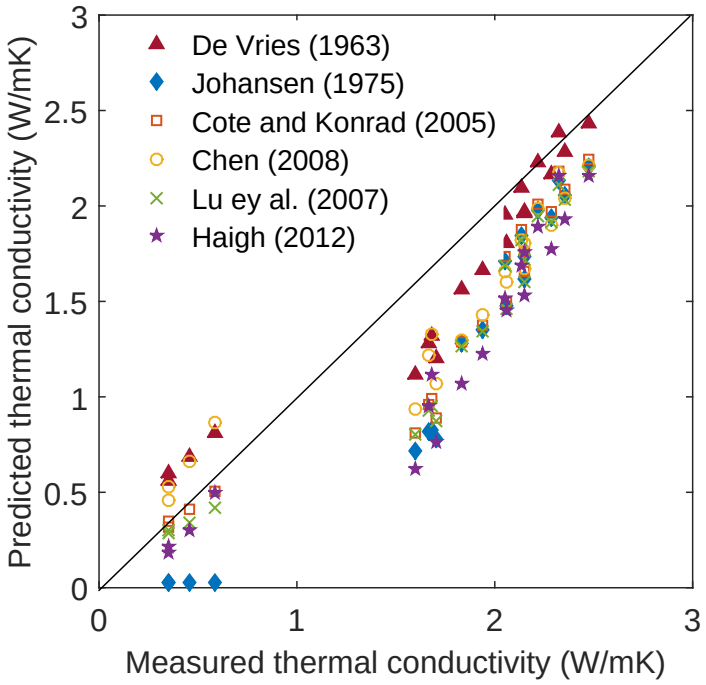

Figure 9: Measured thermal conductivity versus predicted values.

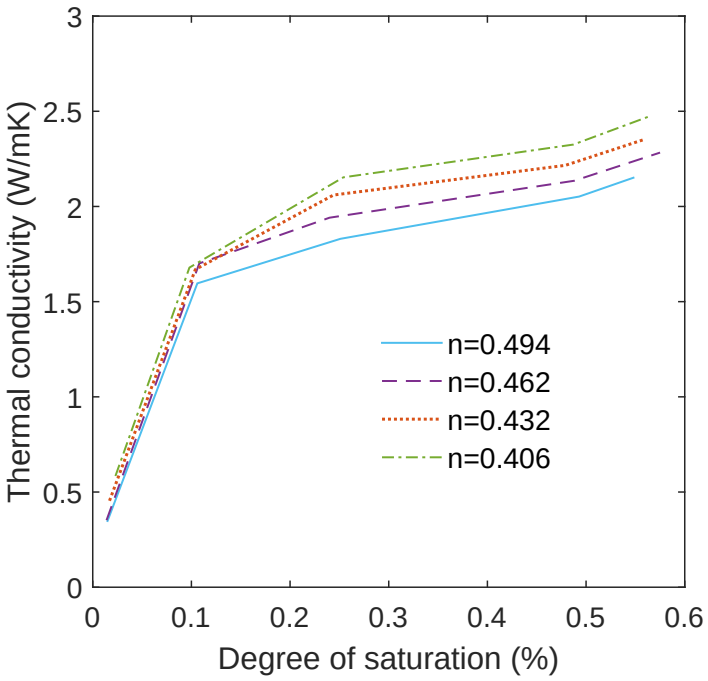

Figure 10: Thermal conductivity versus degree of saturation at different porosities.

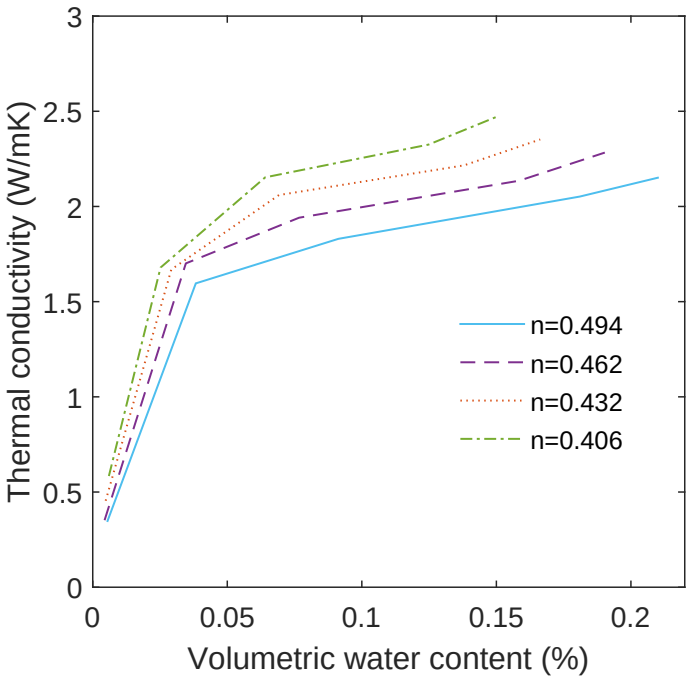

Figure 11: Thermal conductivity versus volumetric water content at different porosities.

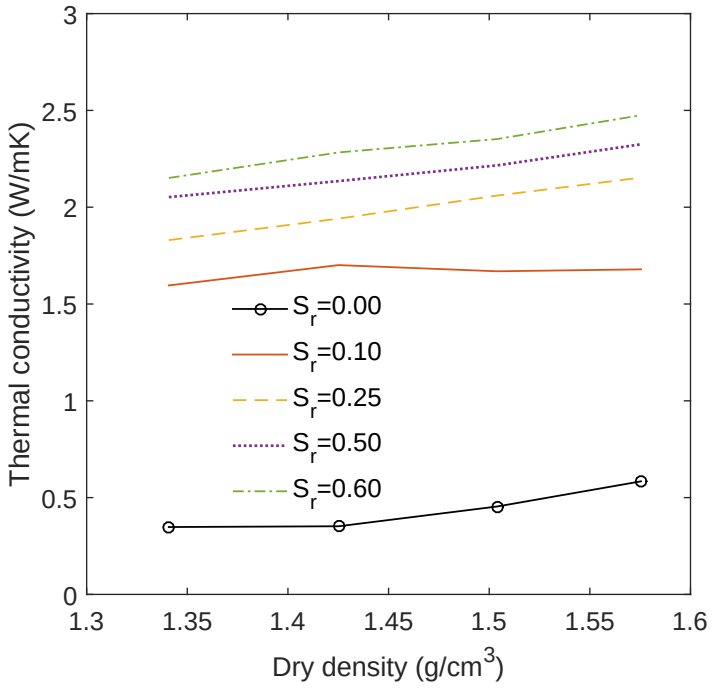

Figure 12: Thermal conductivity versus dry density at different porosities.

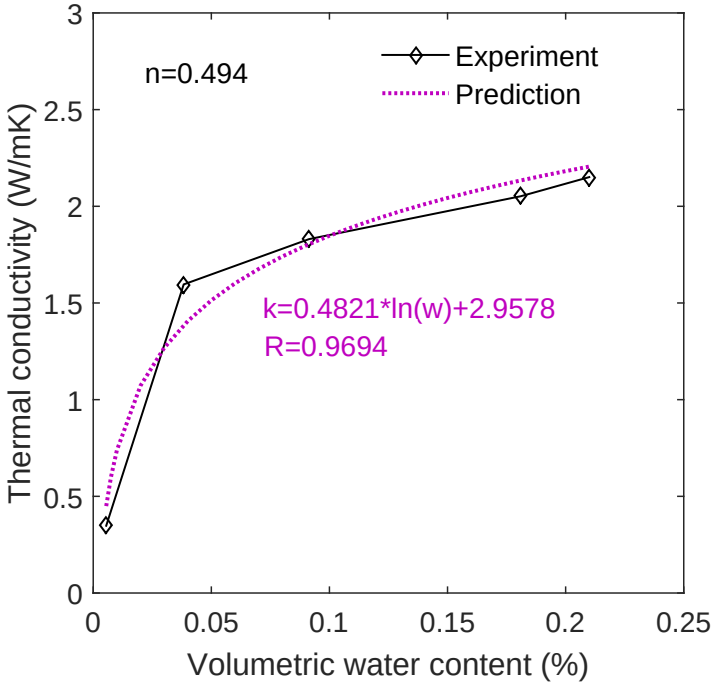

Figure 13: Example of logarithmic variation of thermal conductivity versus volumetric water content.

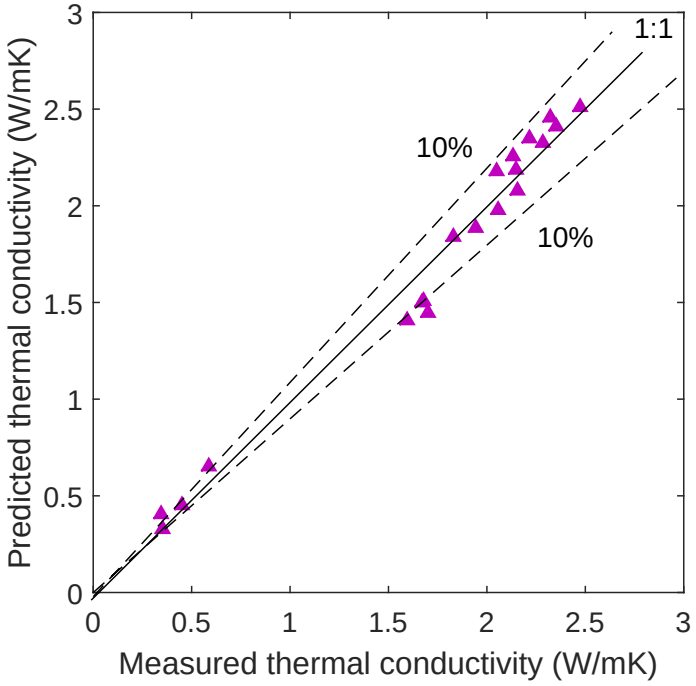

Figure 14: Measured thermal conductivity versus new empirical model results.

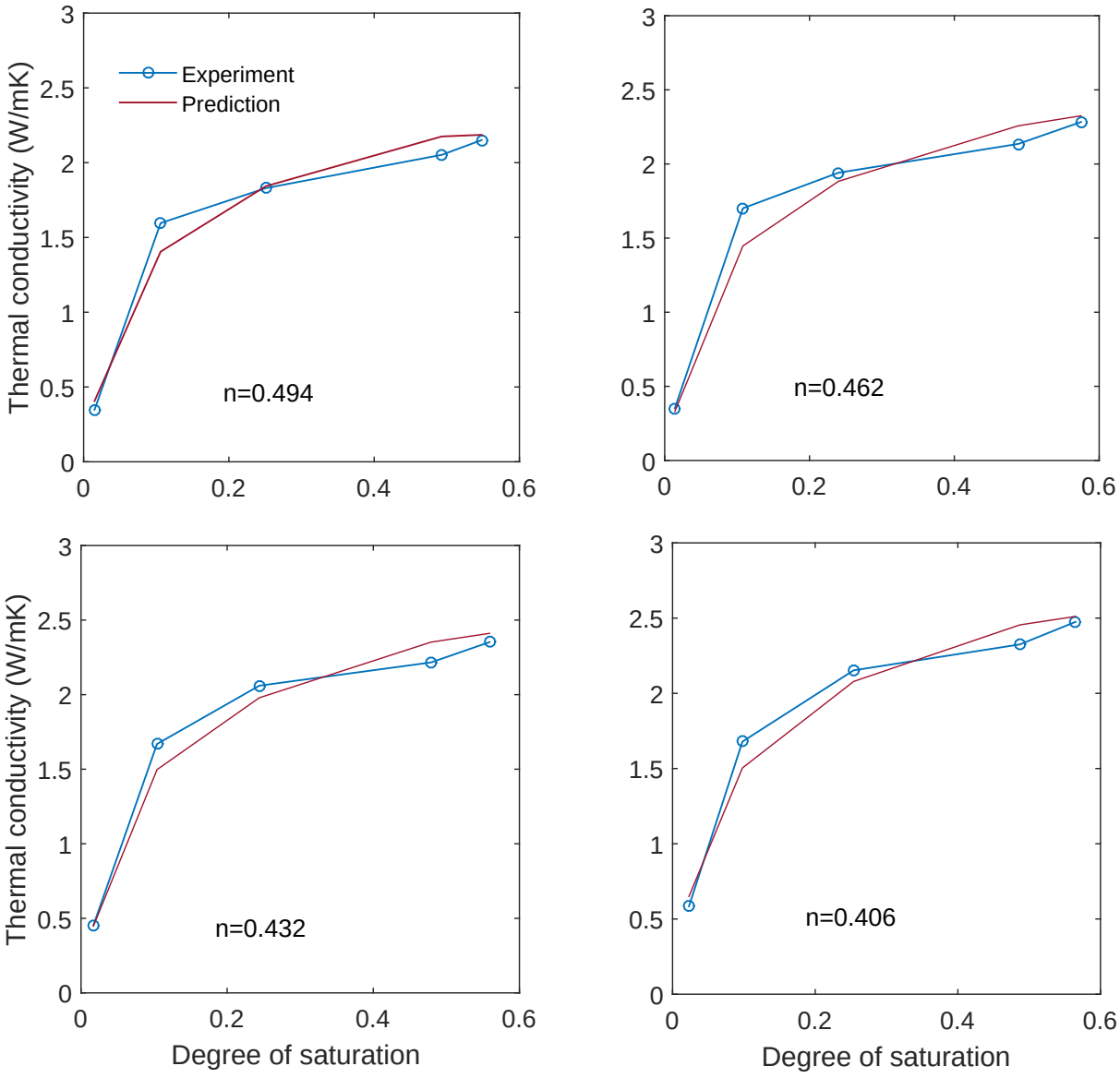

Figure 15: Validation of the new empirical model against experimental results.